Institute for Functional Genomics

L-type Cav1.3 Channels Regulate Ryanodine Receptor-dependent Ca^{2+} Release during Sino-Atrial Node Pacemaker Activity

Angelo Giovanni Torrente[a-d], Pietro Mesirca[a-c,*], Patricia Neco[e-g,*], Riccardo Rizzetto[a-c, e-h], Stefan Dubel[a-c], Christian Barrere[a-c], Martina Sinegger-Brauns[h], Joerg Striessnig[h], Sylvain Richard[e-f], Joël Nargeot[a-c], Ana Maria Gomez[e-g], Matteo Elia Mangoni[a-c]

[a]CNRS, UMR-5203, Institut de Génomique Fonctionnelle, Département de Physiologie, F-34000 Montpellier, France. [b]INSERM, 1191, F-34000 Montpellier, France. [c]Université de Montpellier, UMR-5203, F-34000 Montpellier, France. [d]Current address: Heart institute Cedars Sinai, Los Angeles, USA . [e]INSERM, U1046, Montpellier, France. [f]CNRS UMR 9214, PhyMedExp, University of Montpellier, France. [g]UMR-S 1180, Inserm, Univ. Paris-Sud, Université Paris-Saclay, Châtenay-Malabry, France. [h]Department of Pharmacology and Toxicology, Institute of Pharmacy; Center for Molecular Biosciences, University of Innsbruck, Austria. (*) P.M. and P.N. contributed equally to this work

Introduction and purpose of the study

Aims: Sino-atrial node (SAN) automaticity is an essential mechanism of heart rate generation that is still not completely understood. Recent studies highlighted the importance of intracellular Ca^{2+} ($[Ca^{2+}]_i$) dynamics during SAN pacemaker activity. Nevertheless, the functional role of voltage-dependent L-type Ca^{2+} channels in controlling SAN $[Ca^{2+}]_i$ release is largely unexplored. Since $Ca_v1.3$ is the predominant L-type Ca^{2+} channel isoform in SAN cells, we studied $[Ca^{2+}]_i$ dynamics in isolated cells and *ex vivo* SAN preparations explanted from wild-type (WT) and $Ca_v1.3$ knockout (KO) mice ($Ca_v1.3^{-/-}$). **Methods and results:** We found that $Ca_v1.3$ deficiency strongly impaired $[Ca^{2+}]_i$ dynamics, reducing the frequency of local $[Ca^{2+}]_i$ release events and preventing their synchronization. This impairment inhibited the generation of Ca^{2+} transients and delayed spontaneous activity. We also used action potentials recorded in WT SAN cells as voltage-clamp commands for $Ca_v1.3^{-/-}$ cells. Although these experiments showed abolished Ca^{2+} entry through L-type Ca^{2+} channel in the diastolic depolarization range of KO SAN cells, their sarcoplasmic reticulum Ca^{2+} load remained normal. β-adrenergic stimulation enhanced pacemaking of both genotypes, though $Ca_v1.3^{-/-}$ SAN cells remained slower than WT. Instead, we rescued pacemaker activity in $Ca_v1.3^{-/-}$ SAN cells and intact tissue through caffeine-mediated stimulation of Ca^{2+}-induced Ca^{2+}-release.

Fig. 1: Mechanism of cardiac automatism

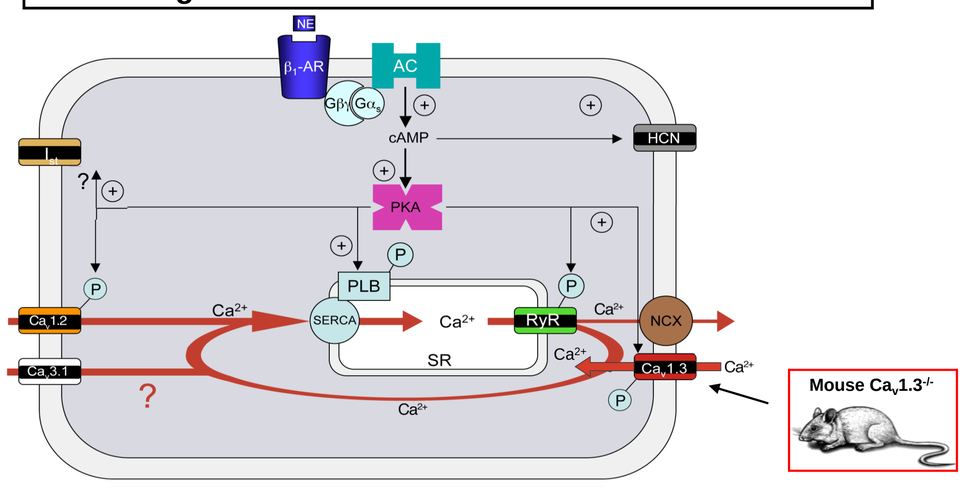

Representative scheme showing all the actors thought to take part in Sinoatrial (SAN) pacemaker activity. This mechanism is probably maintained thanks to the Adenylate-cyclase (AC) activity, which converts ATP in c-AMP. Elevated c-AMP levels have been reported in SAN cells compared to atrial myocites. c-AMP production promotes voltage-dependent opening of f-channels and activates the protein Phospho Kinase A (PKA). PKA phosphorylates different ion channels located on the plasma membrane of pacemaker cells, like L-Type voltage dependent Ca^{2+} channels (LTCC) $Ca_v1.3$ and $Ca_v1.2$ channels. c-AMP –mediated activation of membrane channels, increases their currents inducing in this way the diastolic depolarization of SAN cells. On the other side, high phosphorylation of Phospholamban (PLB) and RyRs increment their open probability, increasing the diastolic concentration of Ca^{2+} and engaging Na^+/Ca^{2+} exchanging (NCX) activity. The inward current generating through this exchange (I_{NCX}), could then help to depolarize SAN cells during the diastolic depolarization phase. β-adrenergic receptor activation further elevates c-AMP and PKA activity, thereby stimulating I_f, $I_{Ca,L}$, RyR and I_{NCX}, which could contribute to the control of the chronotropic state of SAN cells. We hypothesize that $Ca_v1.3$ channels interact with RyRs in order to induce the necessary increase of diastolic Ca^{2+} to activate NCX and contribute to complete SAN diastolic depolarization.

Fig. 2: Spontaneous Action Potentials (Aps) in single SAN cells.

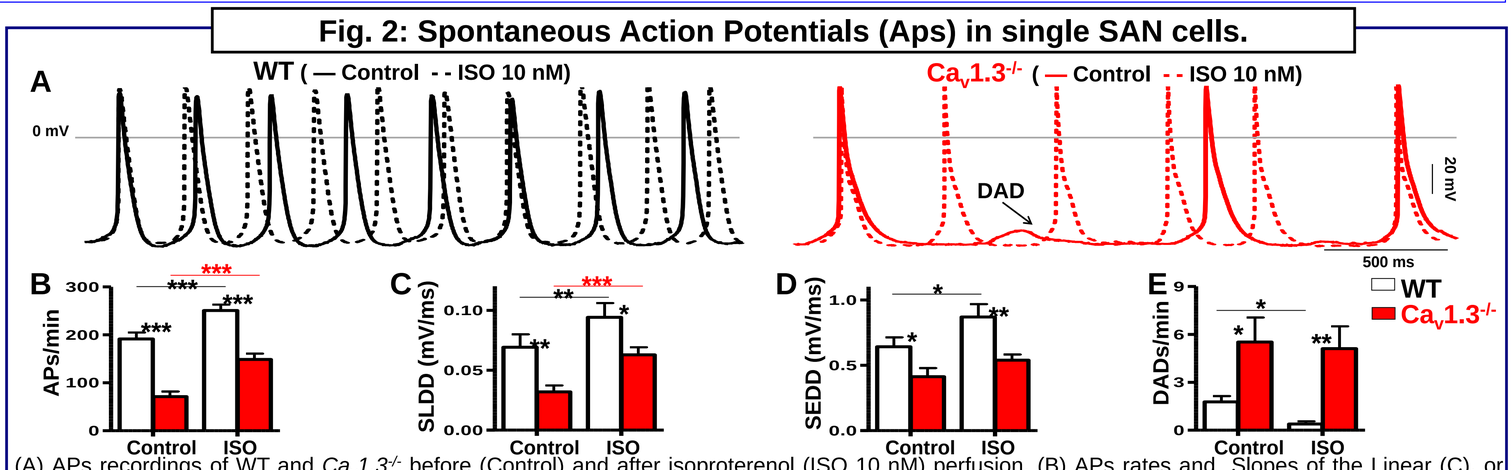

(A) APs recordings of WT and $Ca_v1.3^{-/-}$ before (Control) and after isoproterenol (ISO 10 nM) perfusion. (B) APs rates and Slopes of the Linear (C), or Exponential (D) parts of the Diastolic Depolarization phase (SLDD and SEDD, respectively) in WT (n=17 cells from N=8 mice) and $Ca_v1.3^{-/-}$ (n=22 cells from N=7 mice). (E) Frequency of delayed after depolarizations (DADs) (arrow in (A)) in WT (n=26 cells from N=15 mice) and $Ca_v1.3^{-/-}$ (n=29 cells from N=8 mice). *P<0.05, **P<0.01, ***P<0.001 by 2-way ANOVA with Sidak post-test.

Fig. 3: $[Ca^{2+}]_i$ release in single SAN cells.

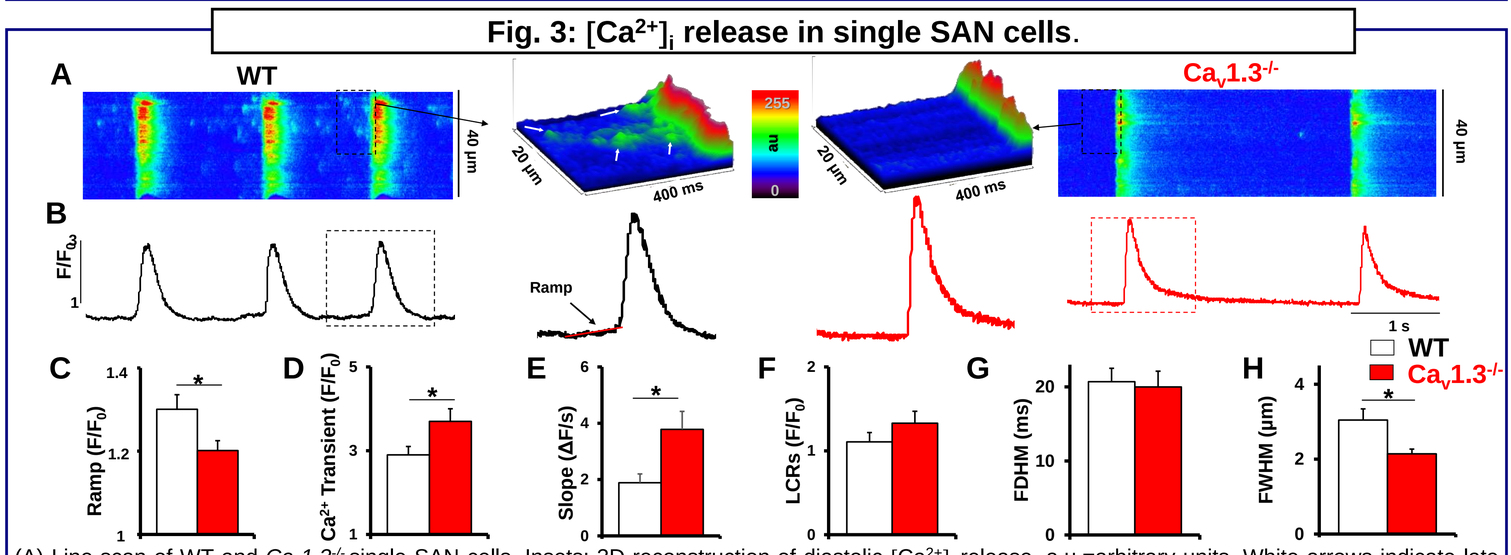

(A) Line-scan of WT and $Ca_v1.3^{-/-}$ single SAN cells. Insets: 3D reconstruction of diastolic $[Ca^{2+}]_i$ release. a.u.=arbitrary units. White arrows indicate late diastolic Local Ca^{2+} Release (LCRs). (B) Time-course of Ca^{2+} fluorescence recorded in (A). Insets: Magnified Ca^{2+} transient of both genotypes. Note the ramp in WT (red line). (C) Amplitude of the ramp in WT (n=10 cells from N=7 mice) and $Ca_v1.3^{-/-}$ (n=13 cells from N=9 mice). (D) Amplitude of the Ca^{2+} transients in WT (n=32 cells from N=16 mice) and $Ca_v1.3^{-/-}$ (n=33 cells from N=16 mice). (E) Slope of Ca^{2+} transient upstroke in WT (n=11 cells from N=6 mice) and $Ca_v1.3^{-/-}$ (n=18 cells from N=6 mice). (F), (G) and (H): amplitude, full duration and full width at half maximum (FDHM and FWHM, respectively) of LCRs recorded in WT (n=10 cells from N=6 mice) and $Ca_v1.3^{-/-}$ (n=19 cells from N=6 mice). *P<0.05 by unpaired t-test.

Fig. 4: Sarcoplasmic Ca^{2+} load in single SAN cells

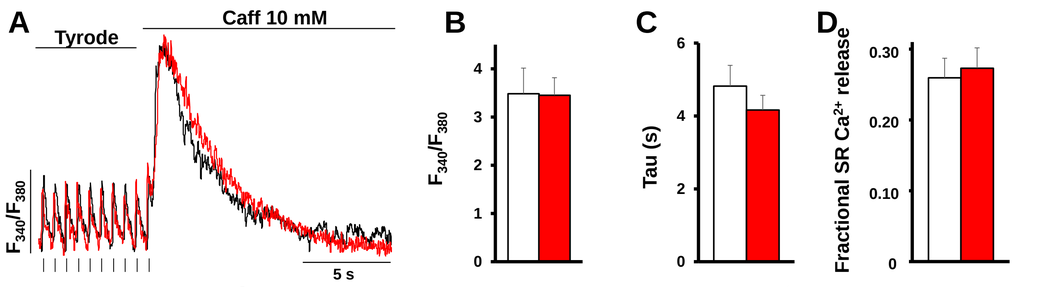

(A) Time-courses of Ca^{2+} fluorescence quantified by Fura 2 in WT and $Ca_v1.3^{-/-}$ single SAN cells, before and after exposure to high concentration of Caff (10 mM). Black ticks indicate electric-field stimulation at 1.5 Hz. (B). (C) and (D): amplitudes, recovery time and fractional SR Ca^{2+} release of the Caffeine (Caff) induced Ca^{2+} transient in WT (n=11 cells from N=3 mice) and $Ca_v1.3^{-/-}$ (n=15 cells from N=3 mice). P=NS by unpaired t-test.

Fig. 6: $[Ca^{2+}]_i$ release in individual cells of the central pacemaker region of the intact SAN. .

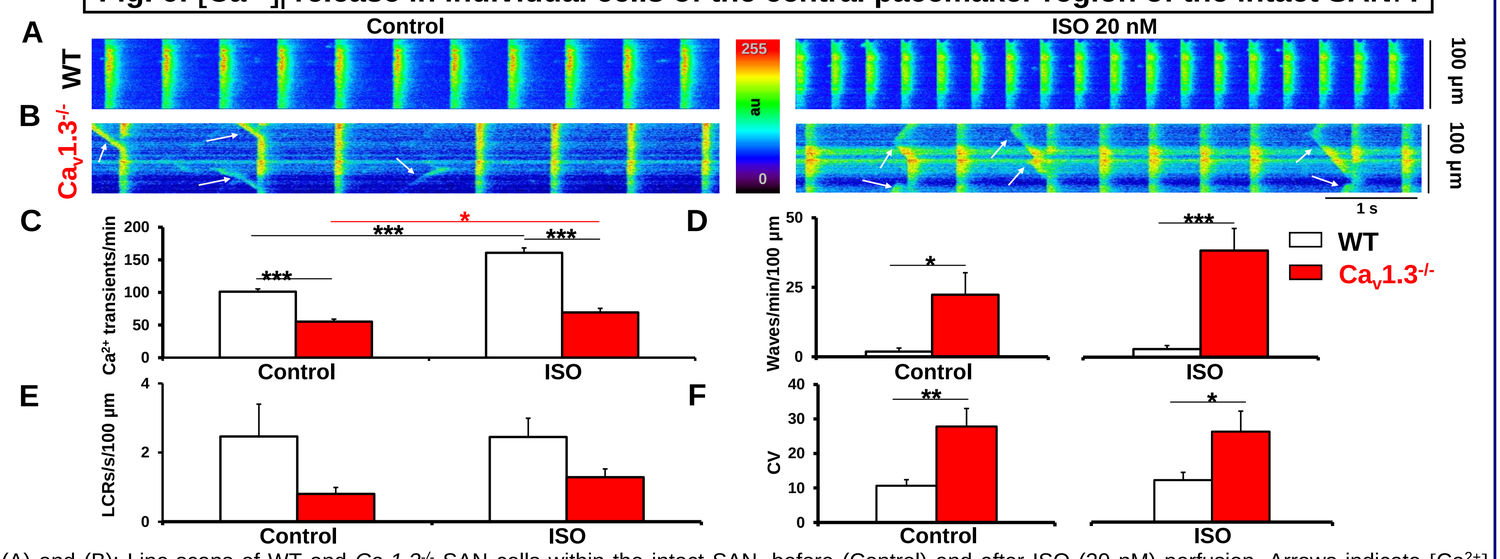

(A) and (B): Line-scans of WT and $Ca_v1.3^{-/-}$ SAN cells within the intact SAN, before (Control) and after ISO (20 nM) perfusion. Arrows indicate $[Ca^{2+}]_i$ waves. Frequency of Ca^{2+} transients (C), $[Ca^{2+}]_i$ waves (D) and Local Ca^{2+} Release (LCRs) (E) in WT (N=5 SAN tissues; at least 3 cells per tissue), and $Ca_v1.3^{-/-}$ (N=9 SAN tissues; at least 3 cells per tissue). (F) Coefficient of variation of Ca^{2+} transient intervals (CV= StD/ mean of cycle length) in WT (n=23 cells in Control and 15 in ISO from N=5 SAN tissues) and $Ca_v1.3^{-/-}$ (n=27 cells in Control and 18 in ISO from N=5 SAN tissues). *P<0.05, **P<0.01, ***P<0.001 by unpaired t-test and 2-way ANOVA with Holm-Sidak's post-test.

Fig. 5: $Ca_v1.3$-mediated $I_{Ca,L}$ activated during the Action Potential cycle

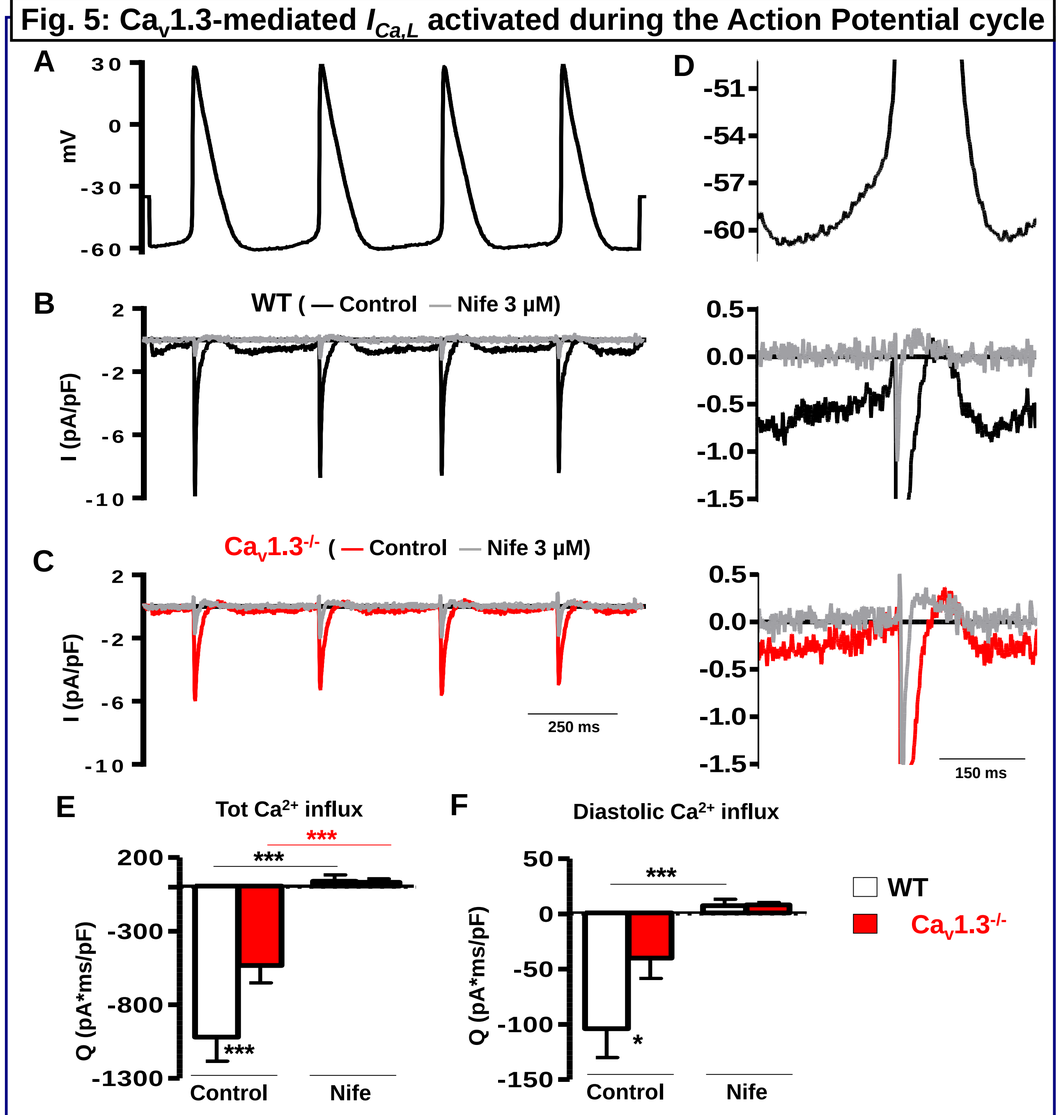

(A) AP samples applied as voltage command. (B) and (C): sample traces of the corresponding net I_{Ca} in WT and $Ca_v1.3^{-/-}$ before (Control) and after nifedipine (Nife, 3 µM) perfusion. (D) Magnification of the second AP of (A) with the respective currents recorded in (B) and (C). (E) Total Ca^{2+} influx via I_{Ca} recorded during the whole AP cycle in WT (n=8 cells from N=3 mice) and $Ca_v1.3^{-/-}$ (n=8 cells from N=2 mice). (F) Diastolic Ca^{2+} influx via I_{Ca} recorded as in (E). *P<0.05, ***P<0.001 by 2-way ANOVA with Sidak post-test.

Fig. 7: Direct conditioning of Ca^{2+} induced Ca^{2+} release by Caffeine.

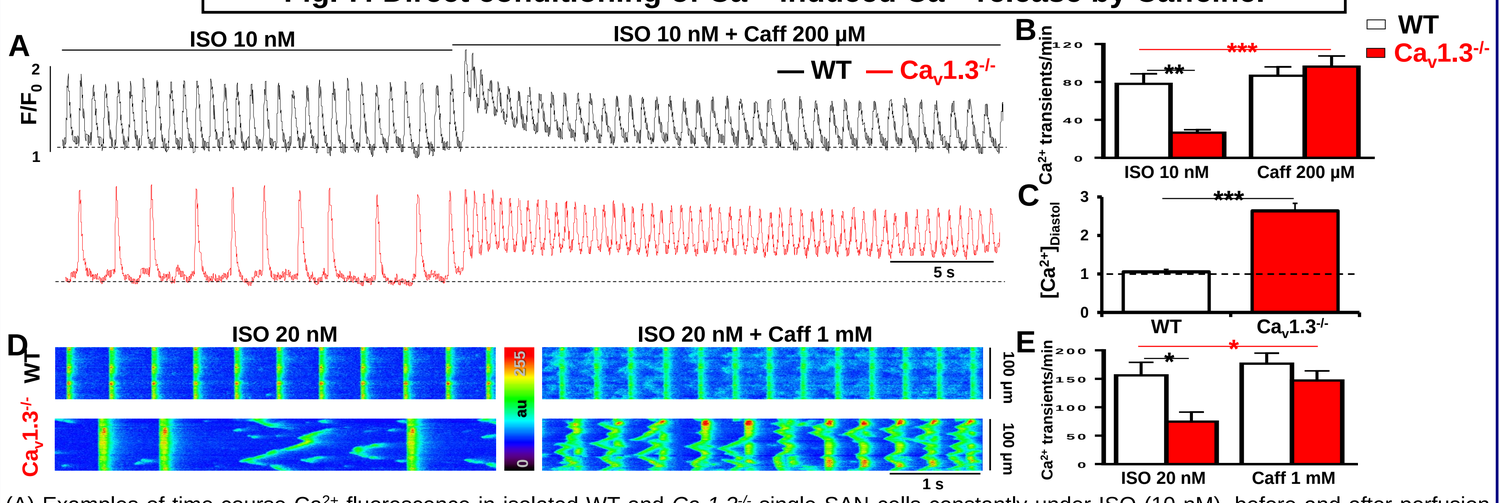

(A) Examples of time-course Ca^{2+} fluorescence in isolated WT and $Ca_v1.3^{-/-}$ single SAN cells constantly under ISO (10 nM), before and after perfusion with low dose of Caffeine (Caff; 200 µM). Dashed lines highlight basal diastolic $[Ca^{2+}]_i$ ($[Ca^{2+}]_{Diastol}$) before Caff (200 µM) perfusion. (B) Frequency of spontaneous Ca^{2+} transients in single WT (n=6 cells from N=4 mice) and $Ca_v1.3^{-/-}$ (n=7 cells from N=3 mice) SAN cells treated as in (A). (C) Line scan recorded in the SAN tissue pacemaker region before and after perfusion with Caff (1 mM). (D) Frequency of spontaneous Ca^{2+} transients in SAN tissue of WT (N=6) and $Ca_v1.3^{-/-}$ (N=8) treated as in (C). *P<0.05, **P<0.01, ***P<0.001 by 2-way ANOVA with Bonferroni's post-test. (E) Changes in $[Ca^{2+}]_{Diastol}$ in WT (n=6 cells from N=4 mice) and $Ca_v1.3^{-/-}$ (n=7 cells from N=3 mice) after perfusion with Caff (200 µM). Values on the Y axis were normalized to the $[Ca^{2+}]_{Diastol}$ (dashed line) measured before Caff (200 µM) perfusion. ***P<0.001 by unpaired t-test.

Conclusions

Our study shows a critical role for $Ca_v1.3$-mediated $I_{Ca,L}$ in regulating $[Ca^{2+}]_i$ release in SAN pacemaker cells. We demonstrated that $Ca_v1.3$ channels stimulate RyR-dependent $[Ca^{2+}]_i$ release during normal SAN pacemaker activity. Given the dual role of $Ca_v1.3$-mediated $I_{Ca,L}$ in driving inward current during the diastolic depolarization phase and in stimulating RyR-dependent $[Ca^{2+}]_i$ release, it is tempting to speculate that these channels constitute an unexplored functional bridge between membrane channels –mediated depolarization (Membrane clock) and Ca^{2+} release –mediated depolarization (Ca^{2+} clock).

Supported by the European Union Research Programme 6th FP MRTN-CT-2006 MRTN-CT-20006-035367